Zhang, Chunhui; Zhang, Yuheng; Xiao, Xiao; Liu, Guoliang; Xu, Zhe; Wang, Bing; Yu, Cunming; Ras, Robin H.A.; Jiang, Lei

Efficient separation of immiscible oil/water mixtures using a perforated lotus leaf

Published in:
Green Chemistry

DOI:
10.1039/c9gc03254a

Published: 01/01/2019

Document Version
Peer-reviewed accepted author manuscript, also known as Final accepted manuscript or Post-print

Please cite the original version:
Zhang, C., Zhang, Y., Xiao, X., Liu, G., Xu, Z., Wang, B., Yu, C., Ras, R. H. A., & Jiang, L. (2019). Efficient separation of immiscible oil/water mixtures using a perforated lotus leaf. *Green Chemistry*, *21*(24), 6579-6584. https://doi.org/10.1039/c9gc03254a

Green Chemistry
Cutting-edge research for a greener sustainable future

Accepted Manuscript

This article can be cited before page numbers have been issued, to do this please use: C. Zhang, Y. Zhang, X. Xiao, G. Liu, Z. Xu, B. Wang, C. Yu, R. H.A. Ras and L. Jiang, *Green Chem.*, 2019, DOI: 10.1039/C9GC03254A.

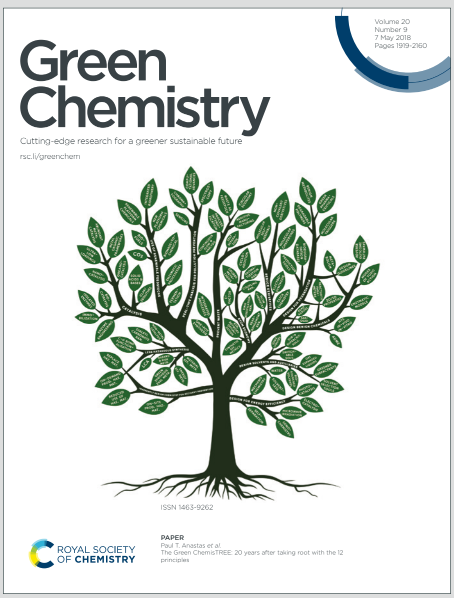

View Article Online
DOI: 10.1039/C9GC03254A

Journal Name

COMMUNICATION

Efficient Separation of Immiscible Oil/Water Mixture *via* Perforated Lotus Leaf†

Chunhui Zhang,‡[ab] Yuheng Zhang,‡[c] Xiao Xiao,[c] Guoliang Liu,[c] Zhe Xu,[c] Bing Wang,[a] Cunming Yu,*[c] Robin H. A. Ras,[de] Lei Jiang[ac]

Received 00th January 20xx,
Accepted 00th January 20xx

DOI: 10.1039/x0xx00000x

www.rsc.org/

Ecosystem and human society are nowadays greatly threatened by oily wastewater or spilled oils. To address these severe issues, considerable advanced methods, such as polymer membrane and polymer-coated mesh with special wettability, have been developed to achieve efficient oil/water separation. However, single superhydrophobic- or superhydrophilic-based membrane or mesh can only permit the oil or water passing through solely, which restricts their applications. Besides, these artificial materials and their fabricating processes may also involve hazardous substances and enormous energy consumption. Therefore, powerful and green oil/water separation approaches are still urgently needed. Herein, we report that the natural lotus leaf with Janus wettability can be a potential candidate for efficient oil/water separation after simple punching by needle. The proposed approach takes advantages of easy-obtained and low-cost natural original material and simple fabrication process, which shows potential applicability to build a greener world.

Oil spill accidents and industrial oily wastewater result in serious environmental pollution and economic losses.[1-3] For example, the Deepwater Horizon oil spill accident in 2010 is regarded as the biggest disaster in exploration of marine oil in history. More than 4.9 million barrels (780000 m^3) of oil was estimated to have leaked into ocean, which caused devastating effects on marine life and enormous economic losses.[4] Thus, addressing these intractable issues, i.e., immiscible oil/water separation, is still urgently needed. With unique wetting properties to oil or water, wettability-based separation techniques have attracted a tremendous amount of attention in both academia and industry.[5-9] For example, in 2004, Feng et al. reported a stainless mesh film coated by polytetrafluoroethylene (PTFE) with unique superhydrophobic and superoleophilic properties, which could efficiently separate the oil/water mixtures.[10] But this type of membrane or mesh can only selectively allow oil ($\rho_{oil} > \rho_{water}$) rather than water to pass through, which results in low separation efficiency of light oil ($\rho_{oil} < \rho_{water}$). In 2011, Xue et al. fabricated a superhydrophilic hydrogel-coated mesh with underwater superoleophobicity, which can let water rather than oil to pass through.[11] This method can separate light oil efficiently but the heavy oil ($\rho_{oil} > \rho_{water}$) will block the mesh and causes reduced separation efficiency. In addition to the above-mentioned methods, various advanced materials with special wettability, in forms of sponges,[12-14] textiles,[15-17] aerogels,[18-20] particles,[21-23] etc., have been prepared for separating oil/water mixtures. Although achieving efficient oil/water separation, these reported methods based on single wettability, i.e. either superhydrophobicity or superhydrophilicity, could only separate one kind of oils (heavy oils or light oils) efficiently. Recently, Liu et al. reported a superhydrophobic–superhydrophilic integrated system, which could be capable of realizing high-flux, high-efficiency, and continuous oil/water separation for both heavy oils and light oils.[24] But this method requires two types of membranes with different wettability and needs a relatively complex device structure. Consequently, efficient separation of heavy oils and light oils by one simple approach still needs to be developed. Membranes or meshes with Janus wettability, i.e., one facet is superhydrophobic and another facet is superhydrophilic should be potential to separate heavy oil or light oils at same time.[25-28] For example, Feng et al. fabricated an integrated mesh with a wettability gradient and achieved dual selective water or oil permeation successfully.[26] Despite that these methods have distinguished performance in separating oil/water mixture, the artificial materials used in these methods still face with two issues: 1)

a. Laboratory of Bio-Inspired Materials and Interface Sciences, Technical Institute of Physics and Chemistry, Chinese Academy of Sciences, Beijing 100190, China.
b. School of Chemical Sciences, University of Chinese Academy of Sciences, Beijing 100049, China.
c. Key Laboratory of Bio-Inspired Smart Interfacial Science and Technology of Ministry of Education, School of Chemistry, Beijing Advanced Innovation Centre for Biomedical Engineering, Beihang University, Beijing 100191, China.
d. Department of Applied Physics, Aalto University School of Science, Puumiehenkuja 2, 02150 Espoo, Finland.
e. Department of Bioproducts and Biosystems, Aalto University School of Chemical Engineering, Kemistintie 1, 02150 Espoo, Finland
E-mail: ycmbhs@iccas.ac.cn
† Electronic Supplementary Information (ESI) available. See DOI: 10.1039/x0xx00000x
‡ These authors contribute equally to this article.

View Article Online
DOI: 10.1039/C9GC03254A

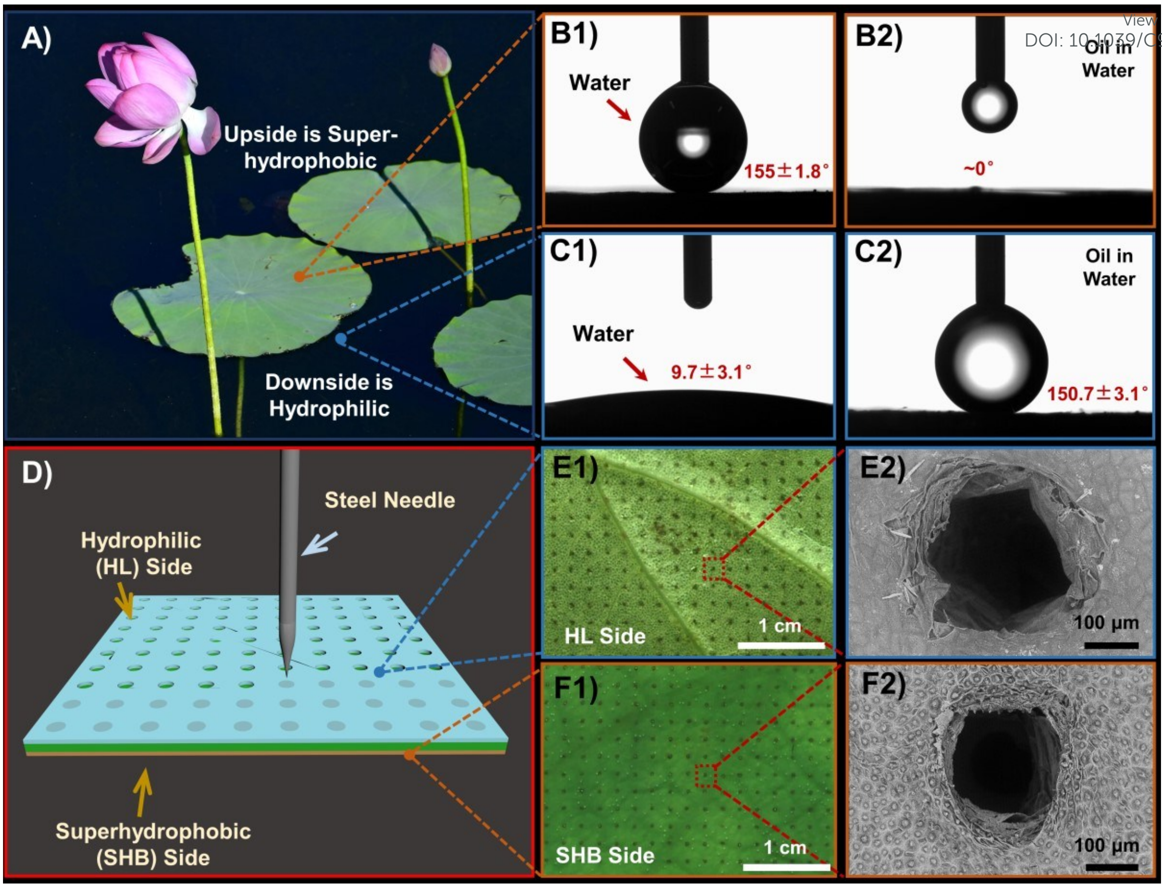

Fig. 1. Illustration of lotus leaf and fabrication process of perforated lotus leaf. A) Optical image of Janus lotus leaf floating on the air-water interface. B1, C1) The WCAs on upside surface and downside surface, respectively. The upside surface is superhydrophobic and the downside surface is hydrophilic. B2, C2) The OCAs on upside surface and downside surface in aqueous environment, respectively. The upside surface is superoleophilic and the downside surface is superoleophobic underwater. D) Mechanical fabrication process of perforated lotus leaf. E1, F1) Optical images of perforated holes on the hydrophilic side (HL side) and the superhydrophobic side (SHB side) of perforated lotus leaf. E2, F2) SEM images of the micro-hole on hydrophilic side and superhydrophobic side.

their fabrication processes usually involve hazardous chemicals; 2) they are not easily degraded in nature, which will result in additional pollution in their disposal process. For example, more than 50 billion litres of wastewater is generated every year and contaminated with solvents such as DMF and NMP during membrane fabrication process.[29, 30] The vast majority of polymers are hard to be degraded and accumulate in landfills or natural environment.[31, 32] Both of these issues do not promote creating a green world. In recent years, a lot efforts have been made in membrane separation science, e.g. biodegradable membranes,[33, 34] recycled membranes,[35] and bioderived solvent used in membrane preparation.[36] However, a simple, low cost, and eco-friendly strategy, that could separate both heavy oils and light oils, is still highly desired in modern society.

After billions of years of evolution, all species in ecosystems have developed co-existence relationships with each other, which have little negative effect on the environment. As is known, natural lotus leaf is capable of stably floating on the air-water interface, even when exposed to wind or rain. This intriguing phenomenon originates from its elegant Janus wettability.[37] As shown in **Figure 1A** and **Figure 1B**, the water contact angle in air (WCA) and oil contact angle underwater (OCA) on the upside surface are 155° ± 1.8° and ~ 0°, respectively, which illustrate the upside surface of lotus leaf is superhydrophobic in air and superoleophilic in water. In contrast, as shown in **Figure 1C**, WCA and OCA on the downside surface are 9.7° ± 3.1° and 150.7° ± 3.1°, respectively, which means the downside surface is hydrophilic in air and superoleophobic in water.[38, 39] The hydrophilic surface can tightly trap water while the superhydrophobic surface repels water, both of which cooperatively endow lotus leaf with the ability of stable floating on the water surface.[37] Herein, taking advantage of the wettability difference between these two surfaces, we demonstrated that the lotus leaf can be a potential candidate for oil/water separation after simple mechanical modification. In this paper, the fresh lotus leaf was selected as the original material. **Figure 1D** schematically illustrates the fabrication process. A needle (diameter of ~ 240 μm) with sharp tip was fixed to a jet dispensing system (details in Method Section and **Figure S1**), which can be precisely manipulated by computer. Through well-controlled punching process, the micro-pore arrays can be successfully obtained, of which diameters (~ 210 μm) are close to the diameter of the needle (**Figure 1E**, **Figure 1F**, and **Figure S2**). We also used the confocal laser scanning microscope to observe the surface structure of upside and downside surface of lotus leaf (**Figure S3**). The

View Article Online
DOI: 10.1039/C9GC03254A

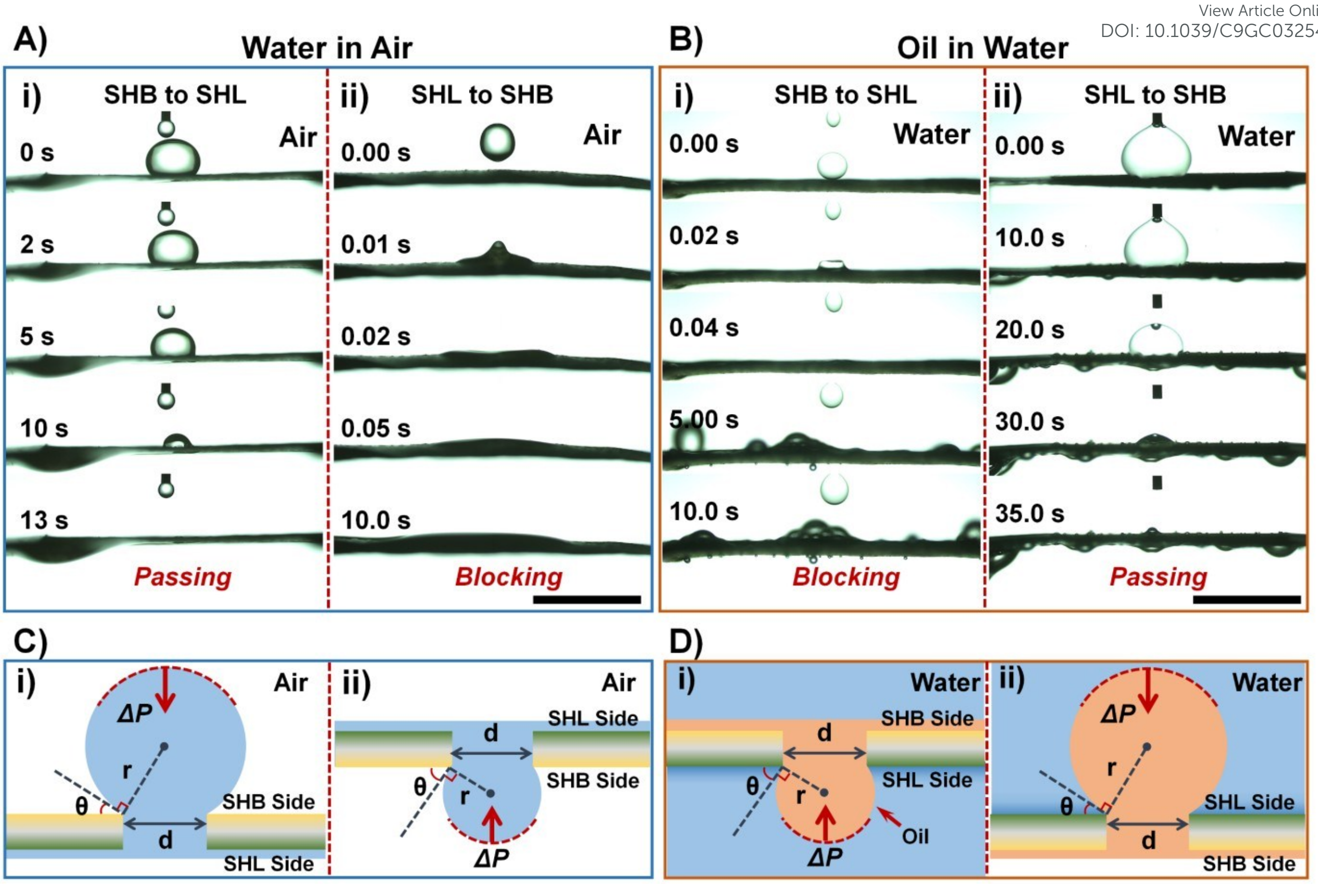

Fig. 2. Unidirectional permeation processes of water/oil droplet and their underlying mechanisms. A) Unidirectional permeation of water in air. Water droplet can spontaneously pass through the perforated lotus leaf from SHB side to SHL side. But in the opposite direction, the water drop cannot pass through the perforated lotus leaf. B) On the contrary, the oil droplet cannot pass through the perforated lotus leaf from SHB side to SHL side whereas successfully permeates from SHL side to SHB side. C, D) Illustration of the mechanism for unidirectional permeation of water and oil, which is mainly attributed to the asymmetric Young-Laplace pressure. Scale bar 1 cm.

hierarchical rough structures could be clearly observed on the upside surface, whereas the downside surface is relatively smooth. SEM image of cross-section is presented in **Figure S4**, which shows the lotus leaf is porous inside. They may also contribute to the flotation of lotus leaf on water surface. During the punching process, the needle might waggle, the leaf tissue might shrink or rupture, resulting in a relatively wide pore size distribution from ~ 110 μm to ~ 270 μm (Figure S2).

To carefully investigate the behaviour of water and oil droplet on the perforated lotus leaf, a high-speed camera (*i*-SPEED 3, OLYMPUS, Japan) was utilized to record their wetting properties. To enhance the hydrophilic property, the downside surface of lotus leaf was pre-wetted by water, of which wettability changed into superhydrophilic (**Figure S5**). As shown in **Figure 2A**, water droplet placed on the superhydrophobic side can gradually penetrate to the superhydrophilic side (Figure 2A-i, **Movie S1**). However, when introduced on the superhydrophilic side, water droplet tends to spread on the superhydrophilic surface rather than penetrate to the superhydrophobic side (Figure 2A-ii, **Movie S2**). The behaviour of oil droplet on perforated lotus leaf can be seen in **Figure 2B**. In this part, dichloromethane was selected to simulate heavy oil's behaviours on the perforated lotus leaf. On the superhydrophobic side, the oil droplet will spread horizontally instead of passing through the lotus leaf (Figure 2B-i, **Movie S3**). When oil droplet is introduced on the superhydrophilic surface, it prefers to pass through the perforated lotus leaf (Figure 2B-ii, **Movie S4**). These phenomena demonstrate the perforated lotus leaf is capable of unidirectional permeation of water and oil droplet. Notably, several air bubbles can be observed when dripping oil droplets on the superhydrophobic surface (Figure 3B). This is because the wetting of oil will destroy the air film between micro-nano structures on the superhydrophobic surface. Then, the destroyed air film will develop into several bubbles (**Figure S6**).

The Janus wettability of lotus leaf is the key factor for the unidirectional permeation of water and oil droplet on perforated lotus leaf. As shown in **Figure 2C-i**, the water droplet on the superhydrophobic surface can be approximately regarded as spherical segment shape, of which volume (V) can be calculated by Equation 1:[40]

$$V = \frac{2}{3}\pi r^3 \left(1 + \frac{3}{2}cos\,\theta - \frac{cos^3\,\theta}{2}\right) \qquad (1)$$

View Article Online
DOI: 10.1039/C9GC03254A

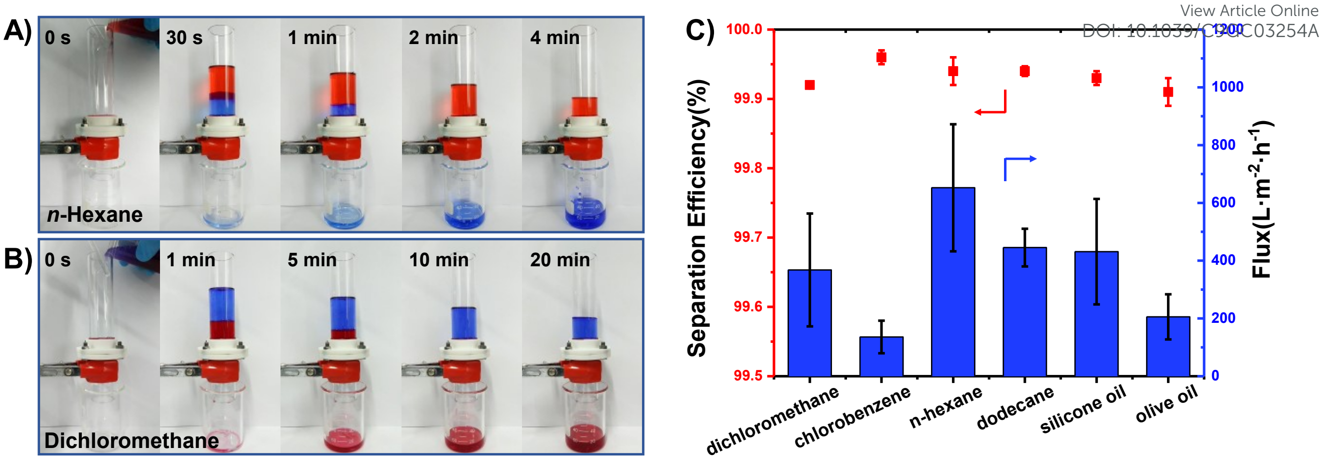

Fig.3. Separation of the mixture of oil (red colour) and water through the perforated lotus leaf. A) The separation processes of the mixture of light oil (n-hexane) and water. B) The separation processes of the mixture of heavy oil (Dichloromethane) and water. C) Separation efficiency and flux of the perforated lotus leaf *versus* different oil/water mixture.

where r is the apparent radius of the water drop, θ is the supplementary angle of WCA. Through this equation, the apparent radius of the droplet can be calculated as follows:

$$r = \left(\frac{V}{\frac{2}{3}\pi + \cos\theta - \frac{\cos^3\theta}{3}}\right)^{\frac{1}{3}} \quad (2)$$

According to Young-Laplace equation, ΔP acting on the curved water droplet can be calculated as follows:[41]

$$\Delta P = \frac{2\gamma}{r} = \frac{2\gamma}{\left(\frac{V}{\frac{2}{3}\pi + \cos\theta - \frac{\cos^3\theta}{3}}\right)^{\frac{1}{3}}} \quad (3)$$

where γ is the surface tension of water. On the pre-wetted superhydrophilic side, the water contact angle is close to 0°, which results in a negligible Laplace pressure. Therefore, under the assistance of ΔP, the water droplet on the superhydrophobic side will be forced to the superhydrophilic side *via* the perforated hole. In contrast, when the perforated lotus leaf is turned over, the Laplace pressure on the superhydrophobic side exhibits a resistance effect to block the permeation of water (Figure 2C-ii). The mechanism of oil's unidirectional permeation on perforated lotus leaf is similar with water droplet (**Figure 2D**). As shown in Figure 2D-ii, there will be a Laplace pressure engendering on oil droplet, when it is placed on the superhydrophilic side, to facilitate its penetration to the superhydrophobic side. Based on the same underlying mechanism, the opposite process, i.e., from superhydrophobic side to superhydrophilic side, is unfavourable.

These interesting phenomena can be also explained from the viewpoint of energy. As shown in **Figure S7**, dripping a water droplet on the superhydrophobic side, the total initial surface energy of water droplet and lotus leaf can be expressed as follows:[42]

$$E_i = (A_i + B_i)\gamma_w \quad (4)$$

where A_i is the surface area of the water-air interface on the superhydrophobic side. B_i is the surface area of the water-air interface on the superhydrophilic side. When the water droplet totally permeated from the superhydrophobic side to the superhydrophilic side, the final total surface energy of water droplet and perforated lotus leaf can be expressed as follows:

$$E_f = (A_f + B_f)\gamma_w \quad (5)$$

Based on Equations 4 and 5, the difference in surface energy (ΔE) can be presented as follows:

$$\Delta E = E_f - E_i = (A_f - A_i)\gamma_w + (B_f - B_i)\gamma_w \quad (6)$$

For a water drop with 10 μL volume, its WCA on the superhydrophobic side is 155±1.8°. Based on the calculation formula of spherical segment area, A_i is about 2.1 × 10^{-5} m^2. A_f is equal to the area of micro-hole, which is about 4.5 × 10^{-8} m^2. B_i and B_f is equal to the surface area of water film on the superhydrophilic side, which could be approximately regarded as constant during permeation process. γ_w is ~ 72 mJ/m^2. According to Equation 6, ΔE is ~ -1.5 × 10^{-6} J.

Notably, our approach is mainly for the separation of immiscible oil/water mixture, which will spontaneously become two phases during the separation process (**Figure S8**). These kind of oil/water mixtures also cause serious environmental disasters, e.g. Deepwater Horizon oil spill accident, which take wide attentions.[5, 9, 10] To verify the oil/water separation capability for both light and heavy oils, the perforated lotus leaf with 2 mm spacing between the holes was fixed between two Teflon fixtures, which are popularly used in oil/water seperation.[43] **Figure 3A** shows the separation process of *n*-hexane/water mixture (the superhydrophobic facet is upward, **Movie S5**). When the mixture of oil dyed by oil red and water dyed by Methyl blue ($\rho_{oil} < \rho_{water}$) was poured into this device, the oil/water mixture firstly contacts with the superhydrophobic surface of lotus leaf. Due to the unidirectional permeation of oil and water on perforated lotus leaf, only water can quickly pass through and be collected by the beaker. Whereas, oil was blocked by the perforated lotus leaf and stayed at the upper tube. Through simply turning over the oil/water separation devices, i.e., the superhydrophilic side

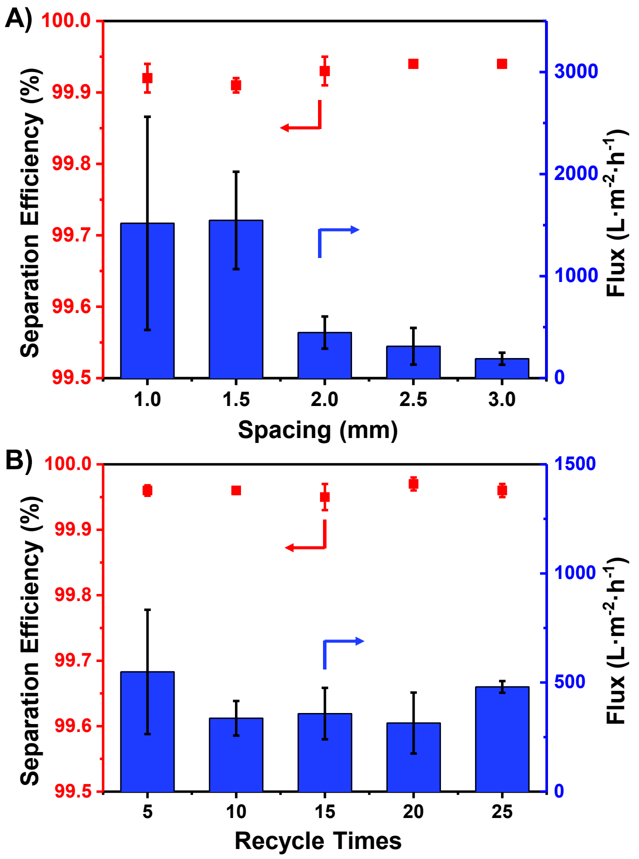

Fig. 4. The effects of the spacing of the micro-hole array and durability of the perforated lotus leaf. A) Variation of separation efficiency and flux with the spacing of the perforated lotus leaf. B) The relationship between the oil/water separation capability (separation efficiency and liquid flux) and the recycling separation time.

is upward, it can realize the separation of heavy oils or organic solvents from water ($\rho_{oil} > \rho_{water}$). As shown in **Figure 3B** and **Movie S6**, dichloromethane can successfully pass through the perforated lotus leaf rather than water. In addition to hexane and dichloromethane, the fabricated perforated lotus leaf also showed distinguished separation performance for chlorobenzene, dodecane, silicone, and olive oil. Silicone oil and olive oil have relatively high viscosity, which demonstrate the perforated lotus leaf could meet the standard of application in high-viscosity environment (**Figure S9**). The perforated lotus leaf illustrates considerable separation fluxes for various oil/water mixtures. The liquid fluxes of the perforated lotus leaf for various oil/water mixtures were assessed by measuring the time of 20 ml oil/water mixtures passing through the lotus leaf. As shown in Figure 3C, the liquid fluxes for dichloromethane/water, chlorobenzene/water, *n*-hexane/water, dodecane/water, silicone oil/water, and olive oil/water, are 367.79 ± 195.39 $L{\cdot}m^{-2}{\cdot}h^{-1}$, 135.95 ± 56.40 $L{\cdot}m^{-2}{\cdot}h^{-1}$, 652.31 ± 219.92 $L{\cdot}m^{-2}{\cdot}h^{-1}$, 445.25 ± 65.12 $L{\cdot}m^{-2}{\cdot}h^{-1}$, 431.09 ± 182.61 $L{\cdot}m^{-2}{\cdot}h^{-1}$, 205.51 ± 78.18 $L{\cdot}m^{-2}{\cdot}h^{-1}$, respectively. Notably, the large error of liquid fluxes originates from the variation of individual natural samples, e.g., the thickness of lotus leaf or the distribution and shape of leaf's veins (Figure E1). Although the errors for the flux are significant, the perforated lotus leaf has high and stable separation efficiency, which is mainly determined by the wettability of lotus leaf. The separation efficiency (R) was calculated as follows:[24, 44]

$$R = 1 - \frac{C_s}{C_o}$$

where C_o is the oil concentration of original oil/water mixture and C_s is the oil concentration of water after oil/water separation. As shown in **Figure 3C**, the R for dichloromethane/water, chlorobenzene/water, *n*-hexane/water, dodecane/water, silicone oil/water, and olive oil/water, are 99.92 %, 99.96 %, 99.94 %, 99.93 %, and 99.91 %, respectively. These results demonstrate that the perforated lotus leaf shows elegant separation performance for light oils and organic solvents, heavy oils and organic solvents, and the oils with high viscosity.

Furthermore, we investigated the influence of the spacing between the holes, on the separation efficiency and flux of the perforated lotus leaf. Micro-hole arrays with various spacings can be easily obtained by simply adjusting the punching machine controller (**Figure S10**). Silicone/water mixture was selected as feed solution in this experiment (**Movie S7**, including the details of fabrication of perforated lotus leaf, preparation of feed solution, separation of feed solution and characterization of the filtrates). **Figure 4A** shows high separation efficiencies can be achieved for different spacings of perforated lotus leaf (the red scatter diagram, all the efficiencies are above 99.9%). While, decreasing the spacing of perforated holes could allow enhancing the oil/water separation flux. For example, the average flux value for the spacing of 3.0 mm is about 190.6 $L{\cdot}m^{-2}{\cdot}h^{-1}$. While, the average flux reaches up to ~ 1517.5 $L{\cdot}m^{-2}{\cdot}h^{-1}$ when the spacing is 1.0 mm. The perforated lotus leaf also demonstrates outstanding durability for oil/water separation. As shown in **Figure 4B**, after 25 recycle times, the perforated lotus leaf with 2 mm spacing still illustrates stable separation efficiency (> 99.90 %) and high oil/water flux (> 300 $L{\cdot}m^{-2}{\cdot}h^{-1}$), which shows promising application in practical applications.

Conclusions.

In this contribution, we demonstrated that the natural lotus leaf with Janus wettability, i.e., its upside surface is superhydrophobic while its downside surface is hydrophilic, can be fabricated into an oil/water separation device. After simple punching process, the lotus leaf was facilitated with unidirectional permeation for water and various oils. Both light oils and heavy oils can be successfully separated by the perforated lotus leaf with high separation efficiency and durability. Low spacing of micro-hole array, i.e., large number of micro-holes per square, will result in high separation flux. While, in this case, the separation efficiency still remains at a high level. Furthermore, compared with the artificial oil/water separation methods, e.g., polymer membrane, the lotus leaf is a low cost and natural biodegradable material, which has no negative influence on the environment. We believe the use of materials from nature to solve the intractable issues facing modern society, will stimulate people to develop advanced technologies

View Article Online
DOI: 10.1039/C9GC03254A

to move the society forward by taking inspirations from the biological world.

Conflicts of interest

There are no conflicts to declare.

Acknowledgements

This work was supported by the China Postdoctoral Science Foundation (BX201700020, 2017M620013), the National Natural Science Foundation (21431009, N2016KA0089), and the 111 Project (B14009), European Research Council grant ERC-2016-CoG (725513-SuperRepel) and the Academy of Finland Centres of Excellence Programme 2014–2019.

Notes and references

1. A. A. Al-Majed, A. R. Adebayo and M. E. Hossain, *J. Environ. Manage.*, 2012, **113**, 213-227.
2. T. Dalton and D. Jin, *Mar Pollut Bull*, 2010, **60**, 1939-1945.
3. Z. Nixon, S. Zengel, M. Baker, M. Steinhoff, G. Fricano, S. Rouhani and J. Michel, *Mar. Pollut. Bull.*, 2016, **107**, 170-178.
4. J. Michel, E. H. Owens, S. Zengel, A. Graham, Z. Nixon, T. Allard, W. Holton, P. D. Reimer, A. Lamarche, M. White, N. Rutherford, C. Childs, G. Mauseth, G. Challenger and E. Taylor, *Plos One*, 2013, **8**, e65087.
5. J. Li, L. Yan, H. Li, J. Li, F. Zha and Z. Lei, *RSC Adv.*, 2015, **5**, 53802-53808.
6. T. Zhao, D. Zhang, C. Yu and L. Jiang, *ACS Appl. Mater. Interfaces*, 2016, **8**, 24186-24191.
7. S. Zhang, G. Jiang, S. Gao, H. Jin, Y. Zhu, F. Zhang and J. Jin, *ACS Nano*, 2018, **12**, 795-803.
8. Y. Zhu, W. Xie, F. Zhang, T. Xing and J. Jin, *ACS Appl. Mater. Interfaces*, 2017, **9**, 9603-9613.
9. N. Wang, Y. B. Wang, B. Shang, P. H. Wen, B. Peng and Z. W. Deng, *J. Colloid Interface. Sci.*, 2018, **531**, 300-310.
10. L. Feng, Z. Zhang, Z. Mai, Y. Ma, B. Liu, L. Jiang and D. Zhu, *Angew. Chem. Int. Ed.*, 2004, **43**, 2012-2014.
11. Z. Xue, S. Wang, L. Lin, L. Chen, M. Liu, L. Feng and L. Jiang, *Adv. Mater.*, 2011, **23**, 4270-4273.
12. L. Li, B. Li, L. Wu, X. Zhao and J. Zhang, *Chem. Commun.*, 2014, **50**, 7831-7833.
13. C. Yu, C. Yu, L. Cui, Z. Song, X. Zhao, Y. Ma and L. Jiang, *Adv. Mater. Interfaces*, 2017, **4**, 1600862.
14. L. Zhang, H. Li, X. Lai, X. Su, T. Liang and X. Zeng, *Chem. Eng. J.*, 2017, **316**, 736-743.
15. L. Wang, Y. Zhao, Y. Tian and L. Jiang, *Angew. Chem. Int. Ed.*, 2015, **54**, 14732-14737.
16. L. Hou, L. Wang, N. Wang, F. Guo, J. Liu, Y. Chen, J. Liu, Y. Zhao and L. Jiang, *NPG Asia Mater.*, 2016, **8**, e334.
17. J. Zhang and S. Seeger, *Adv. Funct. Mater.*, 2011, **21**, 4699-4704.
18. Y.-Q. Li, Y. A. Samad, K. Polychronopoulou, S. M. Alhassan and K. Liao, *ACS Sustainable Chem. Eng.*, 2014, **2**, 1492-1497.
19. J. T. Korhonen, M. Kettunen, R. H. Ras and O. Ikkala, *ACS Appl. Mater. Interfaces*, 2011, **3**, 1813-1816.
20. H. Bi, Z. Yin, X. Cao, X. Xie, C. Tan, X. Huang, B. Chen, F. Chen, Q. Yang and X. Bu, *Adv. Mater.*, 2013, **25**, 5916-5921.
21. L. Zhang, L. Li and Z.-M. Dang, *J. Colloid Interface. Sci.*, 2016, **463**, 266-271.
22. E. E. Sann, Y. Pan, Z. Gao, S. Zhan and F. Xia, *Sep. Purif. Technol.*, 2018, **206**, 186-191.
23. Y. Song, J. Zhou, J. Fan, W. Zhai, J. Meng and S. Wang, *Adv. Funct. Mater.*, 2018, **28**, 1802493.
24. J. Liu, L. Wang, F. Y. Guo, L. L. Hou, Y. E. Chen, J. C. Liu, N. Wang, Y. Zhao and L. Jiang, *J. Mater. Chem. A*, 2016, **4**, 4365-4370.
25. H.-C. Yang, Y. Xie, J. Hou, A. K. Cheetham, V. Chen and S. B. Darling, *Adv. Mater.*, 2018, **30**, 1801495.
26. S. Feng, Y. Xing, S. Deng, W. Shang, D. Li, M. Zhang, Y. Hou and Y. Zheng, *Adv. Mater. Interfaces*, 2018, **5**, 1701193.
27. Z. Wang, X. Yang, Z. Cheng, Y. Liu, L. Shao and L. Jiang, *Mater. Horiz.*, 2017, **4**, 701-708.
28. H.-C. Yang, J. Hou, V. Chen and Z.-K. Xu, *Angew. Chem. Int. Ed.*, 2016, **55**, 13398-13407.
29. M. Razali, J. F. Kim, M. Attfield, P. M. Budd, E. Drioli, Y. M. Lee and G. Szekely, *Green Chem.*, 2015, **17**, 5196-5205.
30. G. R. Guillen, Y. Pan, M. Li and E. M. V. Hoek, *Ind. Eng. Chem. Res.*, 2011, **50**, 3798-3817.
31. R. Geyer, J. R. Jambeck and K. L. Law, *Sci. Adv.*, 2017, **3**, e1700782.
32. J. B. Lamb, B. L. Willis, E. A. Fiorenza, C. S. Couch, R. Howard, D. N. Rader, J. D. True, L. A. Kelly, A. Ahmad, J. Jompa and C. D. Harvell, *Science*, 2018, **359**, 460-462.
33. F. Galiano, A. H. Ghanim, K. T. Rashid, T. Marino, S. Simone, Q. F. Alsalhy and A. Figoli, *Clean Technol. Envir.*, 2019, **21**, 109-120.
34. P. H. A. Le, N. A. I. Ayob, C. F. Blanford, N. F. M. Rawi and G. Szekely, *ACS Sustainable Chem. Eng.*, 2019, **7**, 11885-11893.
35. B. A. Pulido, O. S. Habboub, S. L. Aristizabal, G. Szekely and S. P. Nunes, *ACS Appl. Polym. Mater.*, 2019, **1**, 2379-2387.
36. T. Marino, F. Galiano, A. Molino and A. Figoli, *J. Membrane. Sci.*, 2019, **580**, 224-234.
37. Y. Zhao, C. Yu, H. Lan, M. Cao and L. Jiang, *Adv. Funct. Mater.*, 2017, **27**, 1701466.
38. J. Drelich and E. Chibowski, *Langmuir*, 2010, **26**, 18621-18623.
39. A. Tuteja, W. Choi, M. Ma, J. M. Mabry, S. A. Mazzella, G. C. Rutledge, G. H. McKinley and R. E. Cohen, *Science*, 2007, **318**, 1618-1622.
40. M. Cao, K. Li, Z. Dong, C. Yu, S. Yang, C. Song, K. Liu and L. Jiang, *Adv. Funct. Mater.*, 2015, **25**, 4114-4119.
41. T. Young, *Philos. Trans. R. Soc.*, 1805, **95**, 65-87.
42. B.-E. Pinchasik, J. Steinkühler, P. Wuytens, A. G. Skirtach, P. Fratzl and H. Möhwald, *Langmuir*, 2015, **31**, 13734-13742.
43. Z. Xu, L. Wang, C. Yu, K. Li, Y. Tian and L. Jiang, *Adv. Funct. Mater.*, 2018, **28**, 1703970.
44. L. Li, Z. Liu, Q. Zhang, C. Meng, T. Zhang and J. Zhai, *J. Mater. Chem. A*, 2015, **3**, 1279-1286.